Semi-Huber potential function for image segmentation

Osvaldo Gutiérrez Mata, Ismael de la Rosa, Jesús Villa, Efrén González, Nivia Escalante

Doctorado en Ciencias de la Ingeniería
Unidad Académica de Ingeniería Eléctrica
Universidad Autónoma de Zacatecas
Zacatecas, Zac. C. P. 98000

Abstract

In this work, a novel model of Markov random field is presented, named Semi-Huber potential function, applied to image segmentation in presence of noise. The main difference with respect to other models that have been taken as a reference, is that the number of parameters in the proposed model is significatively smaller. The idea is to choose adequate parameter values heuristically for a good segmentation of the image. In that sense, experiment results show that the proposed model allows a faster and easier parameter adjustment with razonable computation times.

1 Introduction.

Segmentation is the first step in many image processing applications. Some of them comprise industrial quality control, medicine, robot navigation, geophysical exploration, military applications, agriculture, among others. Image segmentation is an image processing method that subdivides an image into its constitutive regions or objects. However, digital images are usually affected by some degrading factors as blurring or noise coming from image acquisition systems, resulting in degraded or distorted images and, as a consequence, yielding inadequate segmentation results. A degradation process can be described as a degradation function H that, together with an additive noise term n, it operates on an input image x and produces a degraded image y:

$$y = Hx + n. \tag{1}$$

Given y, some previous knowledge about the degradation function and some knowledge about the additive noise term, the aim is to obtain an estimation $\widehat{x}$ of the original image x for a good segmentation of the regions or objects into it [1].

In general, segmentation methods are based on two basic properties of the pixels in relation to their local neighborhood, *discontinuity* and *similarity* [2, 3]. Unfortunately, these both techniques often fail to produce accurate segmentation in presence of noise. To overcome these difficulties, the use of Markov random fields (MRF's) within a Bayesian framework has become a powerful method and has been used in different works and different areas [4], [6]-[15] because enables posing this problem, and many others in image processing, as statistical estimation problems [8] and can capture spatial interaction among pixels, where the solution is going to be estimated from the degraded image.

Usually, information data (input image) is not enough for an accurate estimation of the original image, so the regularization of the problem is necessary. This means that a priori information or assumptions about the structure of x need to be introduced in the estimation process [12]. The a priori knowledge is given in terms of a probability distribution that, together with a probabilistic description of the noise that corrupts the observations, allows the use of Bayes theory to compute the posterior distribution, which represents the likelihood of a solution x given the observations y [16].

Statistical methods look for the solution that best matches the probabilistic behavior of the data. Maximum a posteriori (MAP) estimation allows the introduction of a prior distribution that reflects knowledge or beliefs concerning the types of images acceptable as estimates of the original one [4]. There is a wide variety of MRF models; the difference between them lies on the choice of a potential function. Each of them characterizes the interactions between pixels in the same local group.

In this work, we introduce a novel potential function named *semi Huber* MRF as a proposal of a new algorithm for image segmentation. The main advantage of this model lies in the fact that the hyperparameters to be tuned for an adequate result are fewer than those needed by other models that were taken as a reference to verify the results of the proposed one. Section 2 provides an overview about the Bayesian approach, include a theoretical basis of Markov random fields and describes the MAP estimators used in this work, including the proposed model. Some results and comments for image seg-

mentation experiments are presented in section 3. Finally, in section 4 we give some conclusions.

2 Markov random fields and MAP estimation.

Let $\mathbb{S} = \{(i,j)|1 \leq i \leq m, 1 \leq j \leq n\}$ be the set of sites of a rectangular lattice for a 2D image of $m \times n$ size. Its elements correspond to the locations where an image is sampled. The sites in $\mathbb{S}$ are related to one another via a neighborhood system defined as $\mathbb{N} = \{\mathbb{N}_i | i \in \mathbb{S}\}$. A *clique* c is defined as a subset of sites in $\mathbb{S}$ that consist of either a single site, a pair of neighboring sites, a triple of neighboring sites, and so on [19]. $\mathbb{X}$ and $\mathbb{Y}$ are going to represent MRF's, $\mathbb{Y}$ is going to represent the MRF for the observed data and y is a specific configuration of the field $\mathbb{Y}$. $\mathbb{X}$ is the MRF for the segmentation map and x is a segmentation configuration of the field $\mathbb{X}$.

A Bayesian model is a statistical description of an estimation problem that consist of three components. First, the *prior model* $p(x)$, is a probabilistic description of the real world or its properties, that we are trying to estimate. Second, the *sensor model* $p(y|x)$, is a description of the behavior of noise or stochastic characteristics that relate the original state x to the sampled input image or sensor values y. These two components are combined to obtain the third component, the *posterior model* $p(x|y)$, which is a probabilistic description of the current estimation of the original scene x, given the observed data y. The model is obtained using the Bayes rule:

$$p(x|y) = \frac{p(y|x)p(x)}{p(y)}. \tag{2}$$

In its usual application [10], Bayesian modeling is used to find the *maximum a posteriori* (MAP) estimate, that is, the value of x that maximizes the conditional probability $p(x|y)$.

$$\begin{aligned} \widehat{x}_{\text{MAP}} &= \arg\max_{x \in \mathbb{X}} \{p(x|y)\} \\ &= \arg\max_{x \in \mathbb{X}} \{\log p(y|x) + \log g(x)\}, \end{aligned} \tag{3}$$

where $g(x)$ is a MRF function that models prior information of the phenomena to be estimated as a probability distribution, $\mathbb{X}$ is the set of pixels capable to maximize $p(x|y)$ and $p(y|x)$ is the likelihood function from y given x [18].

The Hammersley-Clifford theorem establishes the equivalence between Markov random fields and Gibbs random fields [10, 15, 19, 20], so the MRF can be determined by defining the potential function in a Gibbs distribution, whose basic form is given by

$$g(x) = \frac{1}{Z} \exp\left(-\frac{1}{T} U(x)\right), \tag{4}$$

where $Z = \sum_{x \in \mathbb{X}} \exp\left(-\frac{1}{T} U(x)\right)$ is the *partition function* and in practice is a normalization constant value. T is the *temperature* parameter, that controls the sharpness of the distribution [10] and in practice is assumed to be 1 [19]. $U(x) = \sum_{c \in \mathbb{C}} V_c(x)$ is the *energy function* which is determined as a sum of *clique potentials* $V_c(x)$ over all posible cliques $\mathbb{C}$ in the neighborhood [7, 14, 15, 19]. Usually the second order pairwise cliques are selected and the potentials of all non-pairwise cliques are defined to be zeros [15]. In that sense, we will consider in this work simple MRF's based on a second order neighborhood (eight sites) and potential functions of the form $\rho(\lambda(x_i - x_j))$ which act on pairs of sites, where λ is a constant that scales the difference between pixel values.

2.1 Semi-Huber proposal.

For $\log g(x)$ in equation (3), we introduce the Huber-like norm or semi-Huber potential function, which has been used in one dimensional robust estimation problems [21] for the case of non-linear regression. This function has been modified for the two dimensional case according with the following equation:

$$\log g(x) = -\lambda \left(\sum_{\{s,r\} \in \mathbb{C}} b_{sr} \rho_1(x) \right) + \text{c}, \tag{5}$$

where s is the site of interest, r corresponds to the local neighbors, c is a constant term and

$$\rho_1(x) = \frac{\Delta_0^2}{2} \left(\sqrt{1 + \frac{4\varphi_1(x)}{\Delta_0^2}} - 1 \right). \tag{6}$$

Here $\Delta_0 > 0$ is a constant value and $\varphi_1(x) = e^2$ with $e = (x_s - x_r)$.

2.2 Generalized Gaussian MRF (GGMRF).

As proposed by Bouman [5], the potential function for a GGMRF is given by

$$\begin{aligned} \log g(x) = -\lambda^p \left(\sum_{s \in \mathbb{S}} a_s x_s^p + \right. \\ \left. \sum_{\{s,r\} \in \mathbb{C}} b_{sr} |x_s - x_r|^p \right) + \text{c}, \end{aligned} \tag{7}$$

where $a_s \geq 0$ and $b_{sr} > 0$. In practice it is recommended to take $a_s = 0$ for Gaussian noise assumption, thus the unicity of the MAP estimator can be assured, resulting in

$$\log g(x) = -\lambda^p \left(\sum_{\{s,r\} \in \mathbb{C}} b_{sr} |x_s - x_r|^p \right) + \text{c}. \tag{8}$$

The selected value for power p is determinant, since it constrains the convergence speed of the local or global estimator and the quality of the estimated image [18].

2.3 Welsh's potential function.

The Welsh's potential function, proposed by Rivera [12] as a hard redescender potential function with granularity control, is defined as

$$\begin{aligned}\log g(x) = -\lambda \Big(\mu \textstyle\sum_{\{s,r\}\in\mathbb{C}} b_{sr}\varphi_1(x) \\ +(1-\mu)\textstyle\sum_{\{s,r\}\in\mathbb{C}} b_{sr}\rho_2(x)\Big) + \mathrm{c},\end{aligned} \tag{9}$$

where μ is the granularity control parameter,

$$\rho_2(x) = 1 - \frac{1}{2k}\exp(-k\varphi_1(x)), \tag{10}$$

and k is a positive scale parameter for edge preservation.

2.4 Tukey's potential function.

Another hard redescender potential function also proposed by Rivera [12] is the Tukey's potential function with granularity control, given by

$$\begin{aligned}\log g(x) = -\lambda \Big(\mu \textstyle\sum_{\{s,r\}\in\mathbb{C}} b_{sr}\varphi_1(x) \\ +(1-\mu)\textstyle\sum_{\{s,r\}\in\mathbb{C}} b_{sr}\rho_3(x)\Big) + \mathrm{c},\end{aligned} \tag{11}$$

where, in this case

$$\rho_3(x) = \begin{cases} 1-\left(1-(2e/k)^2\right)^3, & \text{for } \frac{e}{k} < \frac{1}{2}, \\ 1, & \text{in other case,}\end{cases} \tag{12}$$

k is also a scale parameter and μ provides the granularity control too.

2.5 MAP estimators.

With equation (3) and the MRF's previously defined, the corresponding MAP estimators are deduced. The MAP estimator for a GGMRF [5] is given by:

$$\begin{aligned}\widehat{x}_{\mathrm{MAP1}} = \arg\min_{x\in\mathbb{X}} \left\{\textstyle\sum_{s\in\mathbb{S}} |y_s - x_s|^q + \right. \\ \left. \sigma^q\lambda^p \textstyle\sum_{\{s,r\}\in\mathbb{C}} b_{s-r}\,|x_s - x_r|^p\right\}.\end{aligned} \tag{13}$$

The minimization problem can be solved from a global or local point of view considering various methods [12, 22, 23, 24]. As global iterative techniques we have the descendent gradient, the conjugate gradient, the Gauss-Seidel, among others. Local minimization techniques work minimizing at each pixel x_s. In this work the Levenberg-Marquardt algorithm was used for local minimization, this is because all the parameters included into the potential functions were chosen heuristically or according with values proposed in references [18].Estimator performance depends on the chosen values for parameters p and q. If $p = q = 2$, we have the Gaussian condition and the estimator is similar to the least-square one. When $p = q = 1$, the criterion is absolute and the estimator converges to the median one; nevertheless, this criterion is not differentiable at zero and it causes instability in the minimization process [18]. The form of the first term in equation (13) depends on the type of noise regarded. For all experiments made in this work we assumed that noise has a Gaussian distribution with mean value μ_n and variance σ_n^2. From this idea, the corresponding value for parameter q is 2.

A second MAP estimator is for the semi-Hubber potential function (5) [18, 21] given by

$$\begin{aligned}\widehat{x}_{\mathrm{MAP2}} = \arg\min_{x\in\mathbb{X}} \left\{\textstyle\sum_{s\in\mathbb{S}} |y_s - x_s|^2 + \right. \\ \left. \lambda \textstyle\sum_{\{s,r\}\in\mathbb{C}} b_{s-r}\rho_1(x)\right\}.\end{aligned} \tag{14}$$

As a third MAP estimator we introduce in equation (3) the Welsh's potential function [12], obtaining

$$\begin{aligned}\widehat{x}_{\mathrm{MAP3}} = \arg\min_{x\in\mathbb{X}} \Big\{\textstyle\sum_{s\in\mathbb{S}} |y_s - x_s|^2 + \lambda\Big(\mu\textstyle\sum_{\{s,r\}\in\mathbb{C}} b_{s-r}\times \\ \varphi_1(x) + (1-\mu)\textstyle\sum_{\{s,r\}\in\mathbb{C}} b_{s-r}\rho_2(x)\Big)\Big\}.\end{aligned} \tag{15}$$

Finally, the last MAP estimator to be used corresponds to the Tukey's potential function [12], which is given by the expression

$$\begin{aligned}\widehat{x}_{\mathrm{MAP4}} = \arg\min_{x\in\mathbb{X}} \Big\{\textstyle\sum_{s\in\mathbb{S}} |y_s - x_s|^2 + \lambda\Big(\mu\textstyle\sum_{\{s,r\}\in\mathbb{C}} b_{s-r}\times \\ \varphi_1(x) + (1-\mu)\textstyle\sum_{\{s,r\}\in\mathbb{C}} b_{s-r}\rho_3(x)\Big)\Big\}.\end{aligned} \tag{16}$$

3 Experiments and results.

We present a set of experiments to show the performance of the proposed model in the segmentation of some images. All the tests was executed on a Mac Pro computer with a 2×2.8 GHz Quad-Core Intel Xeon processor and 2 GB at 800 MHz DDR2 RAM. The first experiment was carried out with an image of the brain, trying to segment in three tissues: gray matter, white matter and cerebrospinal fluid. Figure 1 shows segmentation results of the brain image corrupted by centered Gaussian noise, $n \sim \mathbb{N}(0, I\sigma^2)$. In top raw from left to right we have the original brain image, brain image with noise ($\sigma^2 = 10$), and segmentation result using the GGMRF. In the bottom raw we have the segmentation result using the semi-Huber MRF, segmentation result using the Welsh's MRF and segmentation result using the Tukey's MRF. Table 1 shows computation times taken by each model, and table 2 shows the list of hyperparameters to be tuned. Even

Table 1: Computation times taken by each model of MRF for segmentation of brain image.

IMAGE	MODEL	TIME (s)
brain slice	CAMGG	339.0461
(187 × 161)	Semi-Huber	339.1406
	Tukey	334.0902
	Welch	332.3922

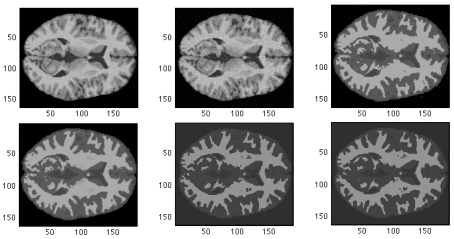

Figure 1: Segmentation of a brain image into three tissues (see text).

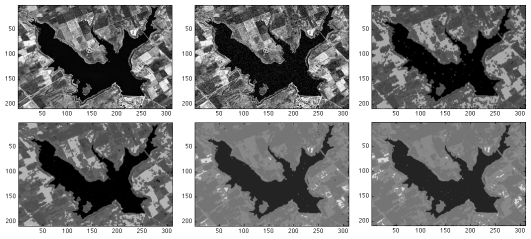

Figure 2: Segmentation of a geographical image into water and no water (see text).

Table 2: List of parameter values for segmentation results in figure 1.

CAMGG	Semi-Huber	Welsh	Tukey
$\sigma = 0.3$	$\Delta_0 = 150$	$\lambda = 10$	$\lambda = 10$
$\lambda = 40$	$\mathrm{X}_0 = 80$	$k = 10$	$k = 10$
$p = 1.5$		$\mu = 0.5$	$\mu = 0.5$
$\mathrm{X}_0 = 80$		$\mathrm{X}_0 = 58$	$\mathrm{X}_0 = 58$

though our proposed model did not yield the shortest time, difference is not significant and visual result is good enough with respect to those obtained with other models. What matters here is that from the original semi-Huber MRF model, we only had to adjust one hyperparameter value, Δ_0 in this case, keeping $\lambda = 1$. Therefore, the number of times that it was necessary to run the segmentation process was significantly lower than with other models.

A second experiment was made with a geographical image of Paso de las Piedras dam, located in Argentina, taken from Google Earth. In this case, the main interest is on segment water from no water in spite of the noise present. Figure 2 shows segmentation results of the dike image. In top raw from left to right we have the original dike image, dike image corrupted by Gaussian noise with $\sigma^2 = 20$, and segmentation result using the GGMRF. In the bottom raw we have the segmentation result using the semi-Huber MRF, segmentation result using the Welsh's MRF and segmentation result using the Tukey's MRF. Table 3 shows computation times taken by each model and table 4 shows the list of hyperparameters values by which results in figure 2 were obtained. Here

Table 3: Computation times taken by each model of MRF for segmentation of dike image.

IMAGE	MODEL	TIME (s)
dike image	CAMGG	704.3832
(310 × 208)	Semi-Huber	713.5470
	Tukey	697.2369
	Welch	704.6216

the semi-Huber proposed model took the longest time; nevertheless, the relative difference is not so big. Also, it can be seen that noise reduction looks more satisfactory than GGMRF model for example, where we can see in the water region, bigger gray points than the others.

Table 4: List of parameter values for segmentation results in figure 2.

CAMGG	Semi-Huber	Welsh	Tukey
$\sigma = 0.4$	$\Delta_0 = 60$	$\lambda = 10$	$\lambda = 10$
$\lambda = 200$	$\mathrm{X}_0 = 90$	$k = 10$	$k = 10$
$p = 1.4$		$\mu = 0.5$	$\mu = 0.5$
$\mathrm{X}_0 = 80$		$\mathrm{X}_0 = 128$	$\mathrm{X}_0 = 128$

4 Conclusions

It was proposed the semi-Huber MRF model to construct a novel algorithm for image segmentation. We verified that this proposal has a satisfactory performance. Times in execution were similar and visual segmentation results were agree with those obtained from models reported in other works. In the case of the Generalized Gaussian, Welsh's and Tukey's Markov random fields, several tests had to be made to find adequate parameter values for each kind of image, since one has more degrees of freedom. While, for the semi-Huber MRF we obtained good results with fewer tests because the parameter adjustment is less complicated. One of the experiments presented was made on a geographical image because we pretend an application on the analysis of this kind of images, properly about hydrographic resources. In this sense, the results are encouraging on this way.

References

[1] R. C. Gonzalez, R. E. Woods, and S. L. Eddins, *Digital Image Processing Using MATLAB*, Prentice Hall, 2004.

[2] X. Cufí, X. Muñoz, J. Freixenet, and J. Martí, "A Review on Image Segmentation Thechniques Integrating Region and Boundary Information", *Advances in Imaging and Electron Physics*, Vol. 120, pp. 1–39, Elsevier, 2003.

[3] M. M. Fernández, "Contribuciones al Análisis Automático y Semiautomático de Ecografía Fetal Tridimensional Mediante Campos Aleatorios de Markov y Contornos Activos. Ayudas al Diagnóstico Precoz de Malformaciones", PhD Thesis, Escuela Técnica Superior de Ingenieros de Telecomunicación, Universidad de Valladolid, November 2001.

[4] K. Sauer, and C. Bouman, "Bayesian Estimation of Transmission Tomograms Using Segmentation Based Optimization", *IEEE Trans. on Nuclear Science*, Vol. 39, No. 4, pp. 1144–1152, 1992.

[5] C. Bouman, and K. Sauer, "A Generalizaed Gaussian Image Model for Edge-Preserving MAP Estimation", *IEEE Trans. on Image Processing*, Vol. 2, No. 3, pp. 296–310, July 1993.

[6] L. Cordero-Grande, *et al*, "Endocarium and Epicardium Contour Modeling Based on Markov Random Fields and Active Contours", *Proc. of the 28th IEEE EMBS Annual International Conference*, New York City, USA, Aug. 30–Sept. 3, 2006.

[7] Y. Zhang, M. Brady, and S. Smith, "Segmentation of Brain MR Images Through a Hidden Markov Random Field Model and the Expectation-Maximization Algorithm", *IEEE Transactions on Medical Imaging*, Vol. 20, No.1, pp. 45–57, January 2001.

[8] S. Krishnamachari, and R. Chellappa, "Multiresolution Gauss-Markov Random Field Models for Texture Segmentation", *IEEE Transactions on Image Processing*, Vol. 6, No. 2, pp. 251–267, February 1997.

[9] D. A. Clausi, and B. Yue, "Comparing Cooccurrence Probabilities and Markov Random Fields for Texture Analysis of SAR Sea Ice Imagery", *IEEE Trans. on Geoscience and Remote Sensing*, Vol. 42, No. 1, pp. 215–228 January 2004.

[10] S. Geman, and C. Geman, "Stochastic relaxation, Gibbs distribution, and the Bayesian restoration of images", *IEEE Trans. Pattern Anal. Machine Intell.*, Vol. PAMI-6, pp. 721–741, November 1984.

[11] S. Z. Li, "MAP Image Restoration and Segmentation by Constrained Optimization", *IEEE Trans. on Image Processing*, Vol. 7, No. 12, pp. 1730–1735, December 1998.

[12] M. Rivera, and J. L. Marroquin, "Efficent half-quadratic regularization with granularity control", *Image and Vision Computing*, Vol. 21, pp. 345–357, 2003.

[13] M. Mignotte, "A Segmentation-Based Regularization Term for Image Deconvolution", *IEEE Trans. on Image Processing*, Vol. 15, No. 7, pp. 1973–1984, July 2006.

[14] H. Deng, and D. A. Clausi, "Unsupervised image segmentation using a simple MRF model with a new implementation scheme", *Pattern Recognition*, Vol. 37, pp. 2323–2335, 2004.

[15] X. Lei, Y. Li, N. Zhao, and Y. Zhang, "Fast segmentation approach for SAR image based on simple Markov random field", *Journal of Systems Engineering and Electronics*, Vol. 21, No. 1, pp. 31–36, February 2010.

[16] J. Marroquin, S. Mitter, and t. Poggio, "Probabilistic Solution of Ill-Posed Problems in Computational Vision", *Journal of the American Statistical Association*, Vol. 82, No. 397, pp. 76–89, March 1987.

[17] R. Szeliski, "Bayesian Modeling of Uncertainty in Low-Level Vision", *International Journal of Computer Vision*, Vol. 5, No. 3, pp. 271-301, 1990.

[18] J. I. de la Rosa, J. J. Villa, and Ma. A. Araiza, "Markovian random fields and comparison between different convex criteria optimization in image restoration", *Proc. XVII International Conference on Electronics, Communications and Computers - CONIELECOMP'07*, Cholula, Puebla, México, February 2007

[19] S. Z. Li, *Markov random field modeling in image analysis*, Springer-Verlag, third edition, 2009.

[20] J. E. Besag, "Spatial interaction and the statistical analysis of lattice systems", *J. Royal Stat. Soc. Ser. B*, Vol. B-36, pp. 192–236, 1974.

[21] J. I. de la Rosa, and G. Fleury, "Bootstrap methods for a measurement estimation problem", *IEEE Trans. on Instrum. Meas.*, Vol. 55, No.3, pp. 820–827, June 2006.

[22] M. Nikolova, and R. Chan, "The equivalence of half-quadratic minimization and the gradient linearization iteration", *IEEE Trans. on Image Processing*, Vol. 16, No.6, pp. 1623–1627, 2007

[23] T. F. Chan, S. Esedoğlu, and M. Nikolova, "Algorithms for finding global minimizers of image segmentation and denoising models", *SIAM Journal of Applied Mathematics*, Vol. 66, No. 5, pp. 1632–1648, 2006.

[24] M. Nikolova, "Functionals for signal and image reconstruction: properties of their minimizers and applications", Research report to obtain the Habilitation à diriger des recherches, Université Paris VI, 2006.